Single-Molecule Spectroscopic Studies of Conjugated Polymers

William L. Miller

Chemistry

Abstract

A semiconductor is a type of material which has electrical properties in between an insulator and a conductor. A conductor can be thought of as a group of atoms surrounded by a sea of free electrons, which are free to move throughout the material; in contrast, the electrons in an insulator are tightly localized on a specific atom or molecule.

In a semiconductor, the electrons are localized as in insulators; however, with the addition of energy, the electrons in semiconductors are easily excited into a state where they are free to move throughout the material as in a conductor. Thus, with the proper combination of materials, electrons can flow from the semiconductor into a circuit when light strikes it. This is the basis behind solar energy, in which a current is generated when sunlight hits silicon-based panels known as photovoltaic cells.

Materials known as conjugated organic polymers are semiconductors made up of elements like carbon, hydrogen, and nitrogen. A polymer is a chain of small repeated units known as monomers. In a conjugated polymer, the electrons of the molecule are shared across several atoms in the polymer; when these electrons are excited, they are then free to move essentially along the entire length of the polymer. Theoretically, then, conjugated polymers could be used for applications like solar energy, as well.

In order to study single conjugated polymer molecules, a technique known as single-molecule spectroscopy (SMS) was used. In SMS, light from a laser is focused to a very small spot ($\sim$10 nm) on a sample composed of individual, isolated single molecules. This laser light excites electrons in the molecules; when the electrons relax back to their ground (lowest-energy) state, they re-release the energy as a characteristic group of wavelengths of light known as a *spectrum*.

I studied the spectroscopy of the conjugated polymers F8BT and MEH-PPV. For F8BT, I studied the effect of polymer size and temperature on the fluorescence of the polymer. The spectrum of F8BT displays a bimodal distribution: some molecules have a peak in their emission spectrum at approximately ∼570 nm ("red"), while some have it at ∼530 nm ("blue").

This bimodal distribution collapses at low temperatures to a single emission peak. Furthermore, small F8BT molecules emit almost entirely in the blue, while many more large F8BT molecules emit in the red form. This indicates that there is some type of low-energy electron "trap" that becomes more abundant as the polymer gets larger. The most commonly-proposed mechanism for this trap is contact between different parts of the polymer chain.

For MEH-PPV, I studied ∼100-molecule aggregates of MEH-PPV polymers. These aggregates contain enough molecules to display characteristics of bulk MEH-PPV with on the order of 10^{23} molecules, but are small enough to be essentially homogeneous – that is, all of the molecules within a single aggregate have identical environments. MEH-PPV shows a similar bimodal emission distribution to that of F8BT; the aggregates emit almost exclusively in the "red" form of MEH-PPV. This further supports the hypothesis that chain-chain contact makes a large contribution to the formation of low-energy traps.

Solar energy production is just one of many areas where conjugated polymers such as F8BT and MEH-PPV could have a huge impact on the world. If good efficiencies can be achieved in converting sunlight into electrical current, things like photovoltaic cells could be much cheaper, easier to produce, and more environmentally friendly.

Contents

1 Introduction and Background

Semiconductors are very important materials that are used in essentially every modern electronic device. Important applications of semiconductors include photovoltaic devices, which convert sunlight into electrical energy, and light-emitting diodes (LEDs), which are efficient and inexpensive devices for light production.[1]

Recently, materials known as conjugated polymers have become widely used for such applications. Conjugated polymers are a class of semiconductors which provide the useful optical and electronic properties of semiconductors combined with the inexpensive and simple processing properties of polymers.[2] Unfortunately, devices made using conjugated polymers exhibit heterogeneous and extremely complex dynamics, which are very difficult to study.

Methods for unraveling these complex dynamics have become available in the past few years, however. In particular, single-molecule spectroscopy (SMS) has been used extensively to examine the optical and electronic properties of single conjugated polymer molecules.[1]

I have studied the optical properties of two conjugated polymers: and poly[9,9-di-*n*-octylfluorene-*alt*-benzothiadiazole] (F8BT) and poly[2-methoxy-5-(2′-ethyl-hexyloxy)-1,4-phenylenevinylene] (MEH-PPV). In particular, I have studied the effects of polymer length and the presence of several molecules on the optical properties of these polymers.

1.1 What Are Semiconductors, and How Are They Useful?

Semiconductors are "between" conductors and insulators; more precisely, they act as insulators, but can be easily excited to act like a conductor when energy is given to them.

Every material has some combination of filled and unfilled electronic energy levels. The highest filled electronic energy level is known as the *valence band* (known as the highest occupied molecular orbital, or HOMO, in organic chemistry), and the lowest unfilled electronic energy level is known as the *conduction band* (lowest unoccupied molecular orbital, or LUMO). The conduction band is named as such because when electrons are excited into this band, they are essentially free to move among the atoms in the metal, and so electricity can be conducted.

In conductors, there is no energy gap (known as a "band gap") between the valence and conduction bands. Therefore, no applied excitation is needed – conductors can always conduct electricity. However, in insulators and semiconductors, there is a band gap energy. Thus, energy must be put into the system (for example, in the form of

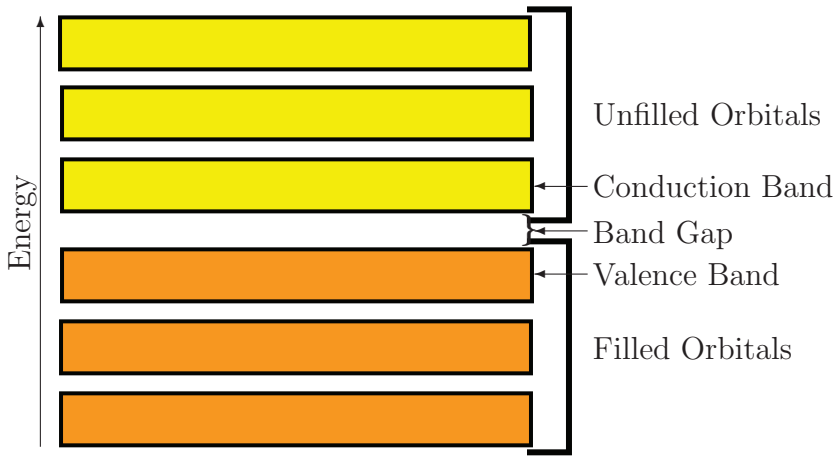

Figure 1.1: A simple diagram of the electronic orbitals in a semiconductor. In a conductor, the band gap is much smaller; in an insulator, it is larger.

electromagnetic radiation) for the material to conduct electricity. See Figure 1.1 for a diagram of a semiconductor band structure.

The difference between insulators and semiconductors is in the size of this gap; insulators have a larger band gap (the cutoff is arbitrarily set at 3-4 eV), and thus it is much more difficult to make them conduct electricity than semiconductors. Many semiconductors have a band gap small enough that electrons can be excited into the conduction band by visible light.

When electrons are promoted to the conduction band in a semiconductor, they leave behind *holes* in the valence band (often represented by h^+). A hole is literally a vacancy in the valence band of the semiconductor with no deeper physical meaning; however, it is often convenient to think of holes as particles which can move throughout the material. A hole "moving" is simply the process of an electron from an adjacent valence band moving into the vacancy; this electron leaves a new vacancy, which is the new location of the

hole.

One particularly important application of semiconductors is in the construction of *diodes*. In a diode, two materials with slightly different conduction band energies are brought together. In most electronics, these two regions consist of silicon with a small amount of "dopant" mixed in to alter its electronic properties. A dopant that easily accepts electrons from the silicon forms a *p-type* region, and a dopant that easily donates electrons to the silicon forms a *n-type* region. The combination of the two is known as a pn junction.

The result of the doping is that the p-type region has an excess of holes (since the dopant molecules have taken some of its electrons) and the n-type region has an excess of electrons. Near the boundary between the two, the electrons in the n-type region can "fall into" the holes in the p-type region – this is generally described as *combination* of an electron and hole. The result is an electrically neutral area known as the "depletion zone" of the diode.

When an electron diffuses into the depletion zone, it sees negatively charged acceptors on the p-type side of the junction (since the acceptor atoms have gained electrons) and positively charged donors on the n-type side. Since an electron has a negative charge, the n-type region is a lower-energy region for the electron than the p-type region; therefore, electrons can easily flow from the p-type to the n-type region, but not the other way around. See Figure 1.2 for a simple diagram of this effect.

A special type of diode, known as a *photodiode*, uses the properties of semiconductors

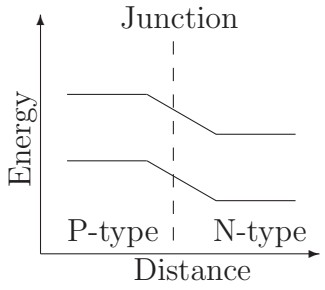

Figure 1.2: A schematic band energy diagram for a traditional diode. The top line in each region is the conduction band, and the bottom line is the valence band.

to produce electricity from sunlight. Generally, the p-type region of the semiconductor is exposed to sunlight. As discussed before, electrons in many semiconductors can be promoted to the conduction band by visible light; thus, the exposure to sunlight promotes some of the p-type region's electrons. Recall, however, that movement from the p-type to the n-type region is "downhill" energetically – thus, promoted electrons in the p-type region eventually diffuse toward the depletion zone, and move into the n-type region.

The n-type region, however, has an excess of electrons – it has very few holes. So this newly added electron from the p-type region has no holes to combine with; it just sits in the conduction band, and a constant flow of such electrons from the p-type region causes the electrons to flow out of the n-type region – a current is generated. To complete the circuit, a conducting wire runs in a grid across the p-type region (on the side facing the sun) to resupply it with electrons.

Another type of diode of particular interest is a *light-emitting diode*, or LED. In an LED, electrons are pumped into the p-type region and holes are pumped into the n-type region. When an electron and a hole meet at the interface between the region, they

combine, releasing energy. This energy is released as light with a wavelength specific to the types of semiconductor and dopant the diode is made of. Thus, a wide range of colored light can be generated from diodes of varying compositions.

1.2 Conjugated Polymers: A Novel Class of Semiconductors

Traditional semiconductors are silicon, germanium, and various alloys (mixtures of elements, at least one of which is a metal). While these types of materials offer very desirable electronic and optical properties, devices made from them can be difficult and expensive to produce. Furthermore, traditional semiconductors are very rigid. *Conjugated polymers* offer an opportunity to solve some of these problems while retaining the important electronic and optical properties of semiconductors.[2]

There are two major types of bonds in chemical compounds. The first two electrons in a bond form a σ bond, which results from direct overlap of electronic orbitals on individual atoms. For example, the p orbitals of two atoms, the "dumbbell" shaped orbitals shown in Figure 1.3(a), form a σ bond by aligning end-to-end as shown in Figure 1.3(b). All additional electrons in a bond (up to 6) pair to form π bonds, which result from side-on overlap of orbitals as shown in Figure 1.3(c).

When a molecule has several alternating single (σ only) and double (one σ and one π) bonds, the electrons in the π bonds become delocalized – they are not bond to one

(a) **(b)** **(c)**

Figure 1.3: **(a)** Two p orbitals. **(b)** A σ bond between two p orbitals. **(c)** A π bond between two p orbitals

specific pair of atoms, but are shared due to π overlap among several atoms in a row. This property is known as *conjugation*.

Conjugated polymers, as the name suggests, are materials with a great deal of conjugation. A polymer is a chain of repeated smaller units known as monomers. There is no strict definition of what these monomers may be; for example, DNA is a polymer made up of nucleotide monomers; polyethylene, an industrially important type of plastic, is simply repeated $-CH_2-CH_2-$ monomers. I have dealt with organic conjugated polymers – an organic material is any material containing the element carbon.

In a conjugated polymer, electrons are shared over several atoms. Therefore, electrons have more freedom than in the average organic polymer. However, they are not able to move freely throughout the entire polymer – so the conjugated polymers are not conductive, either. In fact, conjugated polymers are between insulators and conductors – they are semiconductors.

The two polymers I studied are F8BT and MEH-PPV. Their structures can be seen in Figure 1.4. Notice the presence of alternating single and double bonds, suggesting extensive conjugation.

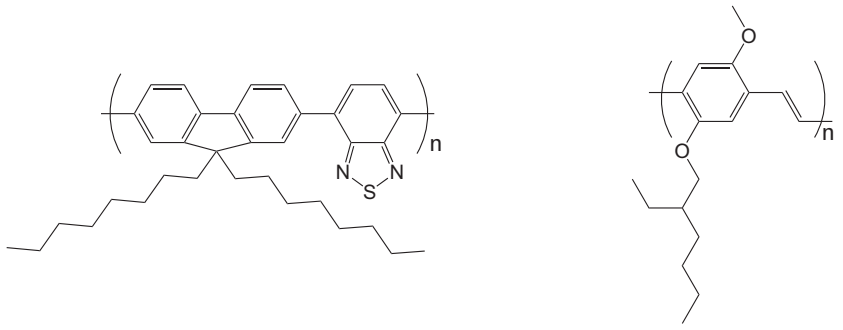

(a) **(b)**

Figure 1.4: Molecular structures of **(a)** F8BT, poly[9,9-di-*n*-octylfluorene-*alt*-benzothiadiazole], and **(b)** MEH-PPV, poly[2-methoxy-5-(2′-ethyl-hexyloxy)-1,4-phenylenevinylene]. Lines represent bonds; any spot where a line ends or two lines meet is a carbon. Hydrogens are implied (not included) in these figures. $(\cdot)_n$ represents repetition of these monomer units n times. For my studies, n is on the order of 1,000 to 10,000.

A particularly useful property of conjugated polymers is that their emission wavelengths can be altered by changing the functional groups attached to the molecule. Functional groups are essentially anything "sticking off" of the polymer chain. It is relatively easy to make polymers with different functional groups - for example, a close relative of MEH-PPV, called DMOS-PPV (poly[2-dimethyloctylsilyl-1,4-phenylenevinylene]) has the same polymer backbone, but different functional groups. It has slightly different optical properties than MEH-PPV while still being comparable in difficulty to produce.[3]

Because they have the properties of semiconductors, organic conjugated polymers can be used to construct products such as photodiodes and LEDs, just as traditional semiconductors can. However, they can be produces at lower cost and with less harm to the environment. One particularly exciting application of organic conjugated polymers is in organic light-emitting diodes, or OLEDs.

In OLEDs, thousands of conjugated polymer diodes are arranged in an array. Because they are so easy to handle, they can actually be "printed" directly onto a substrate in the same way as the ink was printed on this page by an inkjet printer. They can be printed onto any substrate – this is one reason they are so much cheaper than traditional LEDs, which require a specific and expensive type of substrate. If the proper polymers are chosen to yield (for example) red, blue, and green emission, a display monitor is formed. Like many modern displays, OLEDs are very thin, but they have other properties which make them unique.

For example, unlike traditional semiconductor diodes, OLEDs can be printed directly onto thin, flexible plastic substrates, opening the possibility for new products such as roll-up displays. Also, because the pixels of an OLED emit light directly, OLEDs have a better range of colors, brightness, and viewing area. Additionally, they require less electricity input to produce an image than traditional computer monitors such as LCDs.

There are, however, problems in using conjugated polymers in these types of devices; one of the largest is the inherent anisotropy in such systems. Anisotropy is basically "unevenness." A sample is said to be anisotropic if the environments and properties of molecules in the sample vary throughout the sample.

Conjugated polymer systems are very anisotropic. In contrast with traditional semiconductors like silicon, which are composed of one or a simple, predictable mixture of elements, conjugated polymers have several different elements. Some of these elements are chemically bound to each other; others interact with different parts of the polymer

chain (or other chains). Furthermore, conjugated polymers can have a variety of interactions with molecules in the solvent and surrounding air which affect their electronic and optical properties.

1.3 Analysis of Chemical Species Using Spectroscopy

Spectroscopy is the study of matter by examining how different types of energy and matter are emitted, absorbed, or scattered by it. In particular, I excited the molecules using light from a laser source and examined the light emitted from them as their electrons relaxed back to their ground state as a function of wavelength and/or as a function of time.

When a molecule such as a conjugated polymer emits light, it doesn't emit just one specific wavelength (like single atoms do), nor does it emit all wavelengths equally ("white light"). It emits some wavelengths of light much more intensely than others, due to various factors determining the probability of a fluorescence.

One such factor is the probability of the transition. Although the combination of electronic, vibrational, and rotational degrees of freedom in a molecule make a molecule theoretically able to absorb and emit essentially every wavelength of light, some transitions are much more likely than others.

An important rule governing this is called the Franck-Condon principle. This principle states that, because atomic nuclei are several orders of magnitude more massive than electrons, the nuclei of a molecule remain stationary during an electronic transition.[4] The practical consequence of this principle is that an electronic transition can occur much

more easily if the initial and final electronic states result in similar nuclear configurations of the molecule – these transitions are more likely.

In addition to transition probability, another important consideration in determining the emission intensity at various wavelengths is the *quantum yield* of a transition. The quantum yield of an emission phenomenon is the number of times photon emission results from photon absorption.[4] Some electronic transitions may be very likely; however, if they have a low quantum yield, then the electrons are more likely to relax non-radiatively (for example, by releasing heat into the surroundings) than to emit a photon of light.

There is yet another important question about molecular spectroscopy: if the sample is excited with a laser, which emits light with an extremely narrow range of wavelengths, why should any but those wavelengths be observed in the fluorescence (emission) spectrum? If electrons in the molecule are simply being excited and then relaxing back to the ground state, shouldn't the light coming out have the exact same wavelength as the light put in?

The answer is two phenomena known as *vibrational relaxation* and *internal conversion*. The electronic energy levels of a molecule form a sort of a "ladder" climbing in energy, as shown in Figure 1.5. Corresponding to each electronic energy level, there are several associated vibrational levels – these are the lighter lines in Figure 1.5. Visible light can excite a molecule from the ground state (the bottom line) to any vibrational level in a higher electronic state, depending on the excitation energy and the Franck-Condon principle.

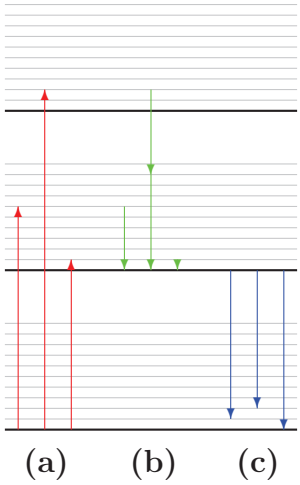

Figure 1.5: An energy band structure for a molecule, showing electronic (dark) and vibrational (light) levels. Some example transitions are shown – **(a)** absorption, **(b)** vibrational relaxation and internal conversion, and **(c)** emission.

However, vibrational transitions are orders of magnitude faster than electronic transitions. So when a molecule is excited into a higher vibrational state, it relaxes nonradiatively almost immediately. This is vibrational relaxation. The molecule then has a different amount of energy to release than it was given. Not only that, but the relaxation of the electron can occur to any of the excited vibrational levels associated with the ground electronic state – again, according to the Franck-Condon principle.

The other process, internal conversion, occurs when the electron makes a nonradiative transition to a lower electronic energy level. Internal conversion processes are not well understood, but they are highly efficient. Thus, the resulting emitted radiation has little relation to the excitation wavelength.

This emitted radiation is, however, closely related to the structure and environment of the molecule. Different environments – different surrounding molecules, for example – can

interact with the molecule so that some energy levels are stabilized, while some are destabilized. Thus, spectroscopy can be (and has been) used extensively for characterization of materials.

Because variables such as the environment affect the electronic properties of conjugated polymers, it is important to understand the complex interactions they have with their environment, including other polymer molecules. These interaction can be probed by spectroscopy. However, in this regard, conjugated polymers pose a much more difficult challenge than traditional semiconductors.

Traditional semiconductors are made of a single metal or a uniform mixture of metals - they are relatively simple and homogeneous. Conjugated polymers, however, are made up of several different elements, bonding to each other in different ways (see Figure 1.4).

Furthermore, polymers are generally produced by "growing" – a small seed monomer or group of monomers known as an oligomer is placed in a solution, and essentially allowed to grow for a specific amount of time. This is not an exact process; the result is a distribution of polymer lengths, which can often be quite large.

Finally, it is important to consider the interactions of the polymers with the substrate used to produce devices. Different substrates will be desirable for different applications, and all will have somewhat different interactions with the molecules very near them. Variables such as the orientation of the molecule relative to the surface and the distance between the surface and the molecule could cause different types of interaction, and thus these variations should be studied.

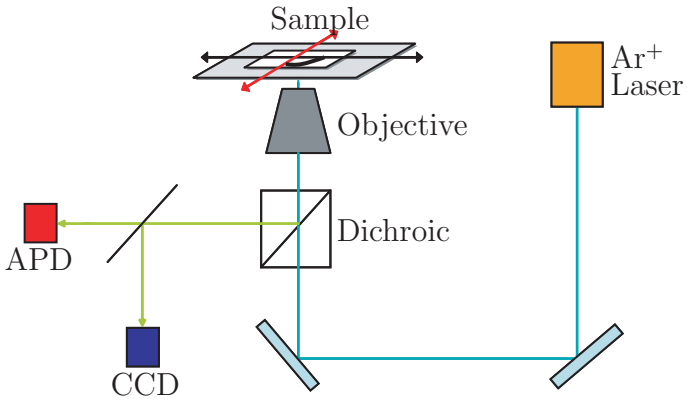

Figure 1.6: Block diagram of a single-molecule spectroscopy apparatus. See text for a thorough explanation.

The variability in properties and environment across a sample is known as "anisotropy." Normal experiments, which examine samples at the macroscopic or microscopic scale, do not have a fine enough resolution to the resolve them, so an average across a large number of molecules is observed. What is needed is a nano-scale (1 nanometer = 10^{-9} meters, the order of the size of individual molecules) technique for analyzing individual conjugated polymer molecules.

1.4 Unraveling Anisotropy Using Single-Molecule Spectroscopy

In *single-molecule spectroscopy* (SMS), as the name suggests, molecules can be examined individually (or in small groups). SMS is performed by *confocal microscopy*; the mechanism is summarized in Figure 1.6. As an excitation source, I used an argon ion (Ar^+) laser. These lasers emit several different wavelengths of radiation; filters can be applied

to reduce the beam to the desired wavelength. Commonly-used wavelengths emitted by an Ar^+ laser are 457.9 nm, 488.0 nm, and 514.5 nm.

This laser excitation light is passed through a dichroic. A dichroic filter allows a narrow band of wavelength to pass through, while reflecting the rest. The light then enters a microscope objective lens, which focuses the laser beam and offers 100× magnification. The light is focused onto the sample, and the sample is moved with nanometer-scale resolution by a two-dimensional translations stage to allow the light to be scanned across the sample surface.

The light emitted from the sample (along with any reflected light) then goes back to the dichroic. This time, the reflected laser excitation is pass back through the filter; the emitted light which is of different wavelengths is reflected at a right angle to the detectors. Generally, before entering the detectors, the light passes through a notch filter, which excludes a very narrow wavelength range (the range containing the laser light). It can then be directed into an avalanche photodiode (APD), a charge-coupled device (CCD), or both (sing an optical instrument known as a beam splitter).

An APD is essentially an extremely sensitive light detector. When a photon strikes a semiconductor material in the APD, that metal releases electrons in a process known as the photoelectric effect. These electrons then strike another semiconductor, which releases several electrons for each electron that hits it. This process repeats through a series of semiconductors, producing a measurable electrical current from even a single photon.

The APD is used to construct an image of the sample. As the translations stage scans the sample over the laser light, the APD measured the emitted light intensity and records it as a function of the position of the light on the sample. Thus, a map of emission intensity is constructed across the sample surface – the molecules are the spots on the sample with significant emission. The APD can also be used to measure a transient, which is simply a plot of emission intensity vs. time. These transients can be surprisingly rich in information.[1]

A CCD is essentially a large array of photodiodes. These photodiodes are not as sensitive as an APD, but are much smaller and less expensive. CCDs are used in digital cameras – colored filters are placed in front of the detectors, so that the color of radiation at each position can be determined by combining the intensities of red, blue, and green light passing through the filters.

For SMS measurements, a monochromator is placed in front of the CCD. A monochromator uses a process called diffraction to spread the light striking it by reflecting it from an extremely fine grating. The light is spread according to wavelength – red (lower-energy) light is diffracted more than blue (higher-energy) light. The resulting spread-out light then strikes the CCD as a line of light. The CCD can be calibrated to recognize the small wavelength range that corresponds to each photodiode along the line. This information can be compiled to produce a *fluorescence spectrum*, which is a plot of light intensity vs. wavelength.

1.5 Recent Work in the SMS of Conjugated Polymers

Conjugated polymers do not exist as simply long, straight rods of monomers. They tend to bend back on themselves, forming complex conformations. My work is concerned primarily with the morphological and packing features of conjugated polymers as single molecules and in small groups. These tend to have important consequences for the electronic and optical properties of the polymers.

Single polymer chains have been modeled using simple simulations known as "bead-on-a-chain" simulations.[5] These simulations showed several distinct possible classes of conformation for the polymers, and experiments using a technique known as single-molecule polarization spectroscopy[5] have been used to specify which of these conformations MEH-PPV adopts. This structure is roughly cylindrical. Because these cylindrical conformations are not spherically symmetrical, there is anisotropy within the molecule – the longer axis might be expected to have different chemical and physical properties than the shorter ones.

In addition to this anisotropy, MEH-PPV contains several "tetrahedral chemical defects," where two different regions of the polymer chain come together and a bond forms between them. These regions are especially important – they draw together carbon atoms from disparate parts of the polymer, allowing π orbital overlap, and thus facilitate intramolecular electron sharing. When an electron is shared among more atoms, it is lower in energy – therefore, these chain-chain contacts are often called "trap" sites. These sites of intramolecular contact are not unique to MEH-PPV – they should be a general

property of conjugated polymer molecules.

I have studied the affect of chain length on spectroscopic properties. In particular, I studied the affect of chain length on the fluorescence properties of F8BT.[6] When SMS studies of F8BT are performed, it turns out that there are two different forms – a "blue" form which has an emission peak at approximately 530 nm, and a "red" form that has a peak at approximately 570 nm.[6,7] This effect has been observed in MEH-PPV as well.[8,9]

It has been hypothesized that the "red," lower-energy emission is caused by energy funneling to the sites of intramolecular contact discussed above. Essentially, when an electron is excited in one part of the molecule, it has relative freedom to move along the length of the chain (due to a conjugated polymer's semiconductor properties). It is drawn to trap sites, and once there, because it is stabilized by the π overlap in the trap, it has less energy than it did when it was excited.

Thus, when it relaxes back to the ground state, the light it emits is lower in energy (has a longer wavelength). To test this hypothesis, polymer of different sizes were examined. Larger polymer molecules should have more intrachain contacts, and thus be more likely to emit in the "red" form.[6] This type of effect has been previously shown in MEH-PPV.[9] Even one low-energy trap site on a molecule should be enough to make it emit in the "red" form.

The affect of temperature was also studied. At 20 K (-253°C), certain modes of vibration along the chain are "frozen out" – the molecule no longer has enough energy to perform those vibrational motions. This results in more ordered π orbital overlap,

and allows electrons to be shared over a longer distance; the result is that the electrons have lower energy. Because of this, low-temperature SMS measurements should reveal a collapse of the bimodal emission character, because the rest of the molecule is essentially brought to the same level energetically as the trap sites.[6]

I also studied the spectroscopic properties of ∼100-molecule aggregates of MEH-PPV. Aggregates are beneficial to study because they combine the complex intermolecular contact of a bulk ($\sim 10^{23}$-molecule) sample with the homogeneity of a single molecule. Because they are only 10-100 nm in size, these polymer aggregates are approximately uniform throughout (there is not enough space for them to vary greatly); however, many properties of bulk samples can be observed.[10]

Because of their large size, MEH-PPV aggregates have a large number of interchain as well as intrachain contacts. These contact points all function as trap sites; the result is that there are no aggregates which lack trap sites, so all aggregates should emit as a low-energy form; there should be no "blue" form of MEH-PPV aggregates.[10]

These studies reveal new information about the electronic and physical properties of conjugated polymer molecules. Hopefully studies such as this will shed light on ways to make conjugated polymers more efficient for the wide variety of applications that have been discussed.

2 Materials and Methods

2.1 Preparation and Analysis of F8BT Single Molecule Samples

F8BT samples of short chain (M_n = 9 kDa, polydispersity index = 3.45) and long chain (M_n = 90 kDa, polydispersity index = 1.99) were synthesized according to Bernius *et al.*,[11] where M_n is the number-averaged molecular weight. The polydispersity index is a measure of the size distribution of the polymer molecules; a perfectly uniform collection of polymer molecules would have a polydispersity index of 1. Dilute thin film samples were prepared by dissolving the samples into a suitable solvent (chloroform) and diluting into a solution of poly(methyl methacrylate) (PMMA, 3% w/w) in toluene.[6]

Solutions were spin-cast onto glass substrates and sealed with gold or aluminum to prevent oxygen from diffusing into the films. Images and spectra were acquired using a scanning confocal microscope (as described in Section 1.4) with the sample temperature regulated by a coldfinger liquid helium cryostat, described in detail elsewhere.[12]

Samples were excited with the 457.9-nm line of an Ar^+ laser, and emitted light was filtered with holographic notch filters to remove scattered excitation and dispersed and detected in a CCD spectrometer. The spectral resolution of the spectrometer was estimated to be ∼3 nm, and because of the invariance of the optics and CCD over the wavelength range used, spectra were not corrected for instrument response. Excitation powers were on the order of ∼0.5-1 μW, corresponding to intensities of ∼200-400 W/cm^2.[6]

2.2 Preparation and Analysis of MEH-PPV Nanoparticle Samples

MEH-PPV nanoparticles were prepared by a reprecipitation method adapted from the literature.[13,14] MEH-PPV (M_n = 186 kDa) was obtained as a gift from the Ferraris group (University of Texas, Dallas) and was dissolved in tetrahydrofuran (THF, Aldrich) at a concentration of ∼10^{-6} M.[10]

Two milliliters of THF solution was added rapidly to 8 mL of deionized water (15 MΩ) while the solution was simultaneously sonicated. MEH-PPV is not soluble in water, and precipitation of nanoparticles occurs rapidly when the THF solution is added to the water. Sonication was continued for an additional 30 min after the addition was complete.[10]

The solution was then heated in a warm water bath to evaporate the THF. The resultant solution was filtered using a 0.1 μm syringe filter (Whatman), yielding a nanoparticle stock solution of particles with a size distribution to be described later. The size distribu-

tion and spectroscopy of the particles of the stock solution were stable for several weeks. Variable molecular weight samples used for SMS studies were prepared as described by Kim *et al.*[12]

Nanoparticle samples in thin films (100 nm thick) of polyvinyl alcohol (PVA, Aldrich) were prepared by spin-coating an aqueous solution of PVA (4%) containing a small aliquot of a freshly prepared nanoparticle stock solution onto a rigorously cleaned microscope cover-slip. Subsequent to spin-coating, the samples were exposed to vacuum for an extended period to remove water and oxygen, followed by evaporation of a gold over-layer to seal the sample and maintain a low concentration of oxygen in the thin film.[10]

Again, data were collected using scanning confocal microscopes. A 488 nm Ar^+ laser line was used to excite the nanoparticles. Excitation intensities were much lower than those used for F8BT single molecules; the excitation power was $\sim$4 W/cm^2. The measurement method and spectral resolution were similar to those for F8BT single molecules.[10]

3 Results

3.1 Size- and Temperature-Dependent Spectroscopic Properties of F8BT Single Molecules

In this study, large numbers of emission spectra of single isolated polymer chains of F8BT at ambient temperature (298 K) and low temperature (20 K) were acquired. Separate samples of short-chain F8BT and long-chain F8BT were studied. All spectra reported herein showed no evidence of flickering or other photoinduced processes during the time in which data were acquired (∼60 s). Typical individual SM spectra for F8BT samples at 20 K are shown in Figure 3.1.

Ensemble spectra were constructed by simply summing the single polymer chain spectra, as shown, for example, in Figure 3.2(b) for long-chain F8BT at 298 K. The spectra were further analyzed by determining the emission energy of the spectral maxima, $E_{\max}$, for each isolated chain. These values were used for two purposes. First, distributions of $E_{\max}$ were determined, e.g., Figure 3.2(a), to obtain insights on the distributions of

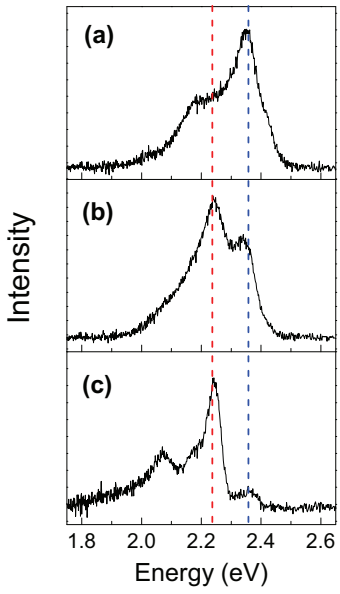

Figure 3.1: Typical single-molecule spectra of long-chain F8BT samples. Spectra are classified according to their wavelength maxima, revealing three forms: **(a)** "blue," **(b)** "mixed," and **(c)** "red."

localized electronic transition energies within the ensemble. Second, the E_{max} values were used as the initial criterion for constructing subensemble spectra (e.g., Figure 3.3), which helped establish the main trends in the data. Interestingly, comparison of long- and short-chain E_{max} distributions from this work and previously reported room-temperature data[7] show virtually identical widths (∼0.2 eV), although both sets of samples had different polydispersities.

All observed spectra exhibit the expected vibronic pattern for a S_1–S_0 (π^*-π) emission transitions in polyfluorene copolymer systems with a dominant progression in a high-frequency C-C stretching vibration (∼0.16 eV).[15] Cursory examination of the single-molecule (SM) spectra for long-chain F8BT reveal anecdotal evidence for the presence a

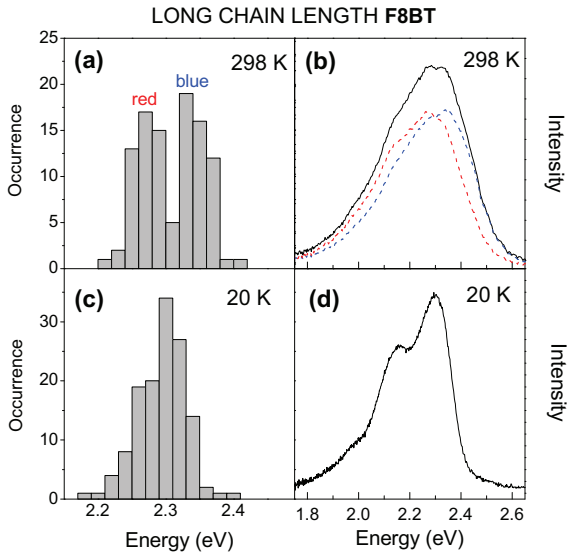

Figure 3.2: Emission peak energy distributions and ensemble (averaged) emission spectra for long-chain F8BT at temperatures of 298 K **(a, b)** and 20 K **(c, d)**. The two components of the bimodal distribution in **(a)** have been labeled "blue" and "red." The dotted spectra in panel **(b)** show sorted subensemble spectra based on the "blue" and "red" $E_{\max}$.

bimodal distribution of spectral maxima, E_{max}. As shown in Figure 3.1, the set of spectra include examples of "blue" spectra, "red" spectra, and mixed (blue and red) spectra. The general trends are analogous to that previously observed for MEH-PPV.[8,9,16] The dual emission properties are emphasized by the vertical dotted lines in Figure 3.1. As described in the Introduction (page 23), low-energy "red" states in conjugated polymers arise from molecular packing effects (chain-chain contacts), which are believed to increase with increasing chain length, leading to lower transition energies for longer polymer chains.

The presence of a bimodal $G(E_{max})$ distribution for long-chain F8BT is especially apparent at 298 K, see Figure 3.2(a). The appearance of distinct peaks for the "blue" and

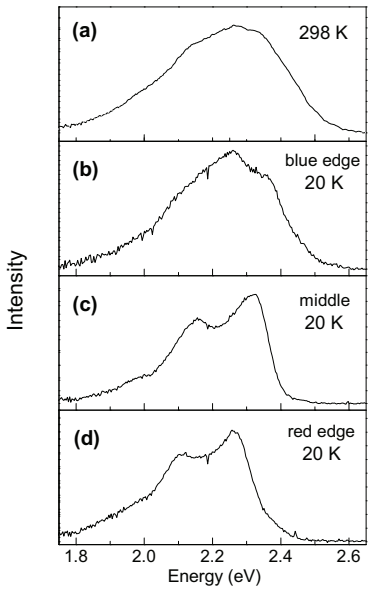

Figure 3.3: **(a)** Ensemble spectra of long-chain F8BT measured at 298 K. Spectra at 20 K were sorted by taking different regions of the peak energy distribution shown in Figure 3.2(c): **(b)** blue edge (2.36–2.42 eV), **(c)** middle (2.30–2.32 eV), and **(d)** red edge (2.17-2.27 eV).

"red" forms for long-chain F8BT in Figure 3.2(a) at 298 K for the host polymer PMMA agrees with a previous observation of long-chain F8BT (M_n = 90 kDa) in a polystyrene host.[15] However, because of lower signal-to-noise ratios for long-chain spectra measured in that work, the bimodal behavior is not as distinct as that shown in Figure 3.2(a).

Surprisingly, a dual peak histogram is not actually observed at low temperature for long-chain F8BT, see Figure 3.2(c). This appears to be due to an overlap of the "red" and "blue" peaks in the distribution. Evidence for this hypothesis is shown in parts (b)–(d) of Figure 3.3, which include subensemble long-chain F8BT spectra at 20 K for the blue, middle, and red portions of the ensemble, respectively. Qualitatively, the vibronic pattern

of the blue subensemble is broader than the other subensembles and has a prominent blue shoulder, suggesting both blue- and red-emitting components

Comparison of the blue regions (ca. 2.3-2.4 eV) of peak energy histograms in Figure 3.2(a) and (c) show that the blue component shifts to lower energy at 20 K and coalesces with the red component, leading to the disappearance of the bimodal distribution. By sorting the 20 K long-chain spectra into subensembles, it is clear that there is not a continuous distribution of peak energies but, rather, overlapping discrete red and blue transitions.

The different temperature dependence of bimodal components was also observed for low-temperature MEH-PPV SM spectra, which was attributed to an increase of effective conjugation lengths at low temperature.[17] This is discussed in more detail in the next section.

Interestingly, the G($E_{\max}$) distribution for short-chain F8BT shows very little evidence for the red-emitting form at 298 or 20 K, see Figure 3.4. Short-chain SM spectra also show broad and unresolved line shapes with lower signal-to-noise ratios than long-chain samples and do not change between 298 and 20 K (data not shown). Apparently, the small chain length prohibits the formation of chain-chain contacts, decreasing the number of red-emitting sites per polymer chain.

This result is consistent with the previous observation that short-chain F6BT (M_n = 9 kDa) also lacked a bimodal distribution and emits exclusively from blue sites.[7] It is also consistent with studies on MEH-PPV that have shown that shorter chains contain a

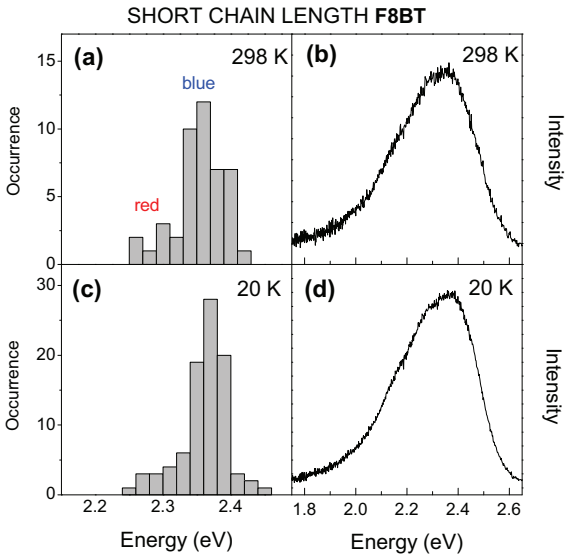

Figure 3.4: Emission peak energy distributions and ensemble emission spectra for short-chain F8BT a 298 K **(a, b)** and 20 K **(c, d)**.

considerably smaller number of red sites.[9] The spectroscopic consequence of chain-chain contacts is even apparent in the 20 K ensemble spectra of F8BT, which are summarized in Figure 3.5.

A comparison of short- (Figure 3.5(a)) and long-chain (Figure 3.5(b)) single-molecule ensemble spectra at 20 K reveal that the latter is significantly shifted to lower emission energies due to red sites. As in the case of MEH-PPV, just a small number of intrachain contacts (even one) is sufficient to funnel the energy to low-energy-emitting chromophores. Figure 3.5(c) portrays an ensemble spectrum of a bulk F8BT film measured at 20 K (which is identical for either short or long polymer chains). This suggests that, in the bulk polymer, interchain contacts are sufficient to efficiently funnel the energy to red sites, and intrachain contacts are not necessary for the red site effect.

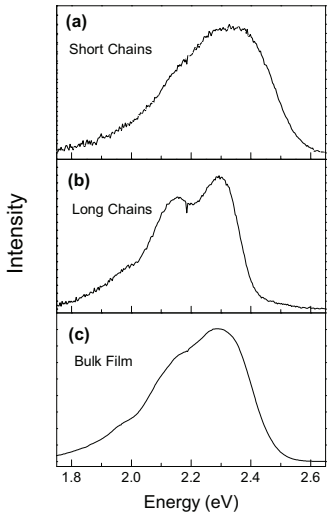

Figure 3.5: Experimental ensemble spectra for short-chain **(a)** and long-chain **(b)** F8BT measured at 20 K. **(c)** Bulk film spectrum measured at 20 K.

3.2 Size-Dependent Spectroscopic Properties of MEH-PPV Nanoparticles

Figure 3.6(a) shows a confocal fluorescence image of an ensemble of assembled nanoparticles of MEH-PPV dissolved in a 100-nm-thick PVA film. The isolated fluorescence spots in the image are due to the individual nanoparticles. Under low intensity ($\sim$4 W/cm^2) irradiation conditions, the spot intensities in the confocal images are highly reproducible with very little evidence of photobleaching, intensity saturation due to the buildup of triplets, or photochemistry

The line scans of the individual spots in the confocal images of the nanoparticles reveal a diffraction-limited spot size (fwhm) of $\sim$300 nm that is indistinguishable from the spot

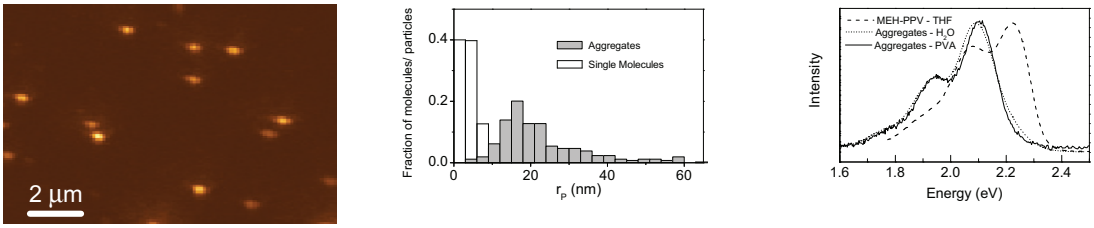

(a) **(b)** **(c)**

Figure 3.6: **(a)** Fluorescence image of single MEH-PPV nanoparticles in a PVA matrix, obtained with 488 nm excitation at an intensity of 50 W/cm^2. **(b)** Estimated distribution of particle radii, r_p, from ∼200 single molecules and nanoparticles. **(c)** Fluorescence emission spectra of MEH-PPV nanoparticles in dilute PVA thin films (solid line), aqueous suspension (dotted line), and in THF (dashed line). The dilute thin film spectrum is the average of ∼75 single nanoparticle aggregate spectra.

size of small single molecules on our apparatus, demonstrating that the nanoparticles are ≪300 nm in diameter.

On the basis of an assumption of constant quantum yield and constant absorption cross section per polymer spectroscopic unit, the spot intensity can be used as an approximate, linear measure of the "particle weight" (PW). The mean fluorescence intensity of an ensemble of isolated single polymer chains with a mean MW of 186,000 amu imaged under the same conditions as the nanoparticle samples was used as a secondary standard leading to the calibration in the bottom axis of the particle intensity histogram shown in Figure 3.6(b).

The size of individual nanoparticles can then be roughly estimated from the particle weight by assuming a spherical shape of the nanoparticles, and a density of 0.8 g/mL, resulting in a rough calibration for the particle radius, r_P . From the above assumptions,

we estimate an r_P of $\sim$20 nm for the nanoparticles, which is in good agreement with the lower size limit established from atomic force microscopy (AFM) measurements.

The emission spectra of an ensemble of nanoparticles at ambient temperature was observed to be insensitive to environment, (e.g., water vs PVA), suggesting that the emission is dominated by the core of the nanoparticles, not the surface. In fact, the assembled nanoparticle samples have an emission spectrum that is very close to bulk thin-film MEH-PPV samples (dashed line in Figure 3.7(f)). The nanoparticle spectra are significantly red-shifted from MEH-PPV dissolved in THF (Figure 3.6(c)), a good solvent for MEH-PPV. This is consistent with expectations that in a good solvent the polymer conformation should be extended without chain-chain contacts, and as a result, lack low-energy sites for singlet excitons.[18,19,20]

The effect of particle size on the frequency-resolved emission spectra is especially apparent in low temperature (20 K) SMS data, as shown in Figure 3.7. Figure 3.7(b), (d), and (f) reveal the evolution of the ensemble spectra as the particle size is increased. Figure 3.7(b) and (d) are ensemble spectra of single polymer chains with molecular weights of 186 and 1,000 kDa, respectively. These data reveal the previously described superposition of emission from high energy blue sites and low energy red sites[18] indicated by the vertical dashed blue and red lines in Figure 3.7. This phenomenon is analogous to the effect described in Section 3.1.

Parts (a) and (c) of Figure 3.7 are histograms of the emission energy maxima of low- and high-MW single molecules whose ensemble spectra are shown in Figure 3.7(b) and

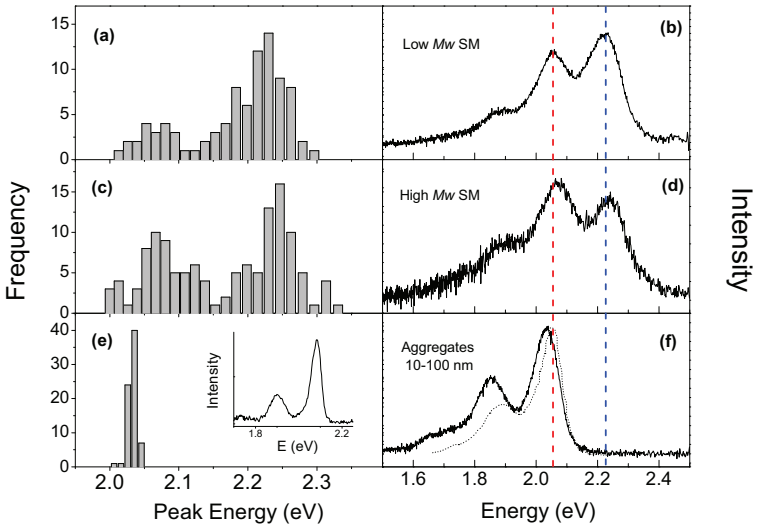

Figure 3.7: Peak wavelength histograms and ensemble emission spectra of MEH-PPV single molecules (SM) and nanoparticle aggregates measured at 20 K; **(a, b)** MW = 186 kDa, **(c, d)** 1000 kDa, and **(e, f)** aggregates. A bulk film MEH-PPV emission spectrum measured at 4K is shown for comparison in **(f)** (dashed line), and the inset in panel **(e)** shows a single nanoparticle spectrum measured at 20 K. The red and blue vertical dashed lines denote the red and blue energy maxima, respectively.

(d), respectively. The vibronic features in the ensemble spectra in Figure 3.7(b) and (d) are significantly broader than the individual single-molecule spectra that were used to construct the ensemble spectra. The broadening is due to molecule-to-molecule conformational and environmental variations.

An example of an individual nanoparticle spectrum is shown in the inset to Figure 3.7(e). Both SM histograms exhibit the previously reported characteristic bimodal distribution behavior[8,18] associated with blue and red sites. The red sites have been assigned previously to dilute low-energy sites along the polymer chain that are excited primarily by energy transfer from the more plentiful blue sites.

Clearly, the ratio of blue- to red-emitting species changes with molecular weight (chain length).[12] The much higher probability of observing emission from the blue sites in the low MW samples is due to the relatively small size of these polymer chains and the presence of very few red sites per chain (in some cases none).

For larger single-molecule chains shown in Figure 3.7(c) and (d), there is a higher probability of a chain possessing a red site (i.e., an increase in chain-chain contacts). As a result, the distribution of emission maxima (Figure 3.7(c)) has nearly equally probable blue-emitting molecules. Although the energy splitting between blue and red forms is close to the dominant progression interval, this feature is purely accidental and is not due to vibronic (false) origins or large emitting-state displacements (Huang-Rhys factors).[12]

Interestingly, assembling several polymer chains together has an enormous effect on the emission spectroscopy. The emission maxima histogram of nanoparticles (Figure 3.7(e)) collapses to a single peak close to the emission maximum of bulk MEH-PPV dominated by red sites. In addition, the ensemble emission spectrum of the assembled nanoparticles closely resembles the spectrum of the bulk thin film (Figure 3.7(e), dashed line), which is in excellent agreement with previous observations in MEH-PPV aggregate systems.[21]

A detailed investigation of different particles in the ensemble revealed that even the smaller assembled nanoparticles exhibit spectra that are dominated by red site emission. The fact that the cores of the assembled nanoparticles are spectroscopically indistinguishable from the bulk thin film suggests that bulk-like structure and properties are achieved for MEH-PPV for particle radii greater than approximately 10 nm.

4 Discussion

4.1 Size- and Temperature-Dependent Spectroscopic Properties of F8BT Single Molecules

Figure 3.1 shows three characteristic long-chain (molecular weight = /sim90,000 amu) single-molecule F8BT spectra. Each of these three spectra represents a group of molecules corresponding to either "red," "mixed," or "blue" peak emission. A similar trend has been described in MEH-PPV.[8,9,16] The mechanism behind this shift was explored.

First, the temperature dependence of F8BT's fluorescence properties was studied. The bimodal distribution disappears at low temperature (see Figure 3.2(a) vs. (c)); evidence for the cause can be found in Figure 3.3. The spectra were sorted into subensembles based on their peak energy; the "blue edge" is particularly informative. This subensemble is much broader than the other two, with a prominent blue shoulder; this suggests the presence of a blue- as well as a red-emitting component.

When the room-temperature and blue-edge low-temperature spectra (Figure 3.3(a) vs.

(b)) are compared, a shift to lower energy is seen for the blue form in moving to lower temperature. Thus, the evidence suggests that the blue component shifts to lower energy and coalesces with the red component at low temperature.

Previous work with MEH-PPV[17] has shown a similar effect; the temperature dependence in this case was attributed to an increase in effective conjugation length at low temperature. The increase in conjugation length is due to the "freezing out" of certain *vibrational modes*; F8BT molecules undergo a huge variety of different vibrational motions, including modes that involve the stretching of bonds, modes that involve *bending*, and modes that involve both.

As discussion in Section 1.2, the emission of a conjugated polymer is sensitive to the degree to which an electron is shared along the chain. It is easy to imagine that the electron could be shared more or less effectively across the length of the molecule depending on, for example, how straight the molecule is. Thus, certain bending modes can actually decrease the degree of conjugation along the chain. This both increases the energy of the electron directly and makes it less likely to be able to travel to a low-energy trap site (discussed below).

But what does this have to do with low-temperature measurements? At low temperatures, some vibrational modes are "frozen out" – there is no longer enough thermal energy to excite these modes. The result is that the conjugation length in the polymer is increased relative to the polymer at room temperature, in which these disruptive bending modes are freely excited by the thermal energy in the surroundings.

Next, fluorescence spectra of short-chain (molecular weight = ∼9,000 amu) F8BT molecules were compared to the long-chain spectra - for example, see Figure 3.2 and Figure 3.4. The most striking difference between these two is the near absence of red sites in the room-temperature peak energy histogram of short-chain F8BT (Figure 3.4(a)).

This is explained by the presence of intrachain contacts, as discussed in Section 1.5. Long-chain F8BT molecules are much more likely to have these contact (simply because there are more opportunities for such to form), so they have a much larger fraction in the "red" form.

In Figure 3.5, (a) short chain, (b) long-chain, and (c) bulk film F8BT emission spectra are compared. All spectra were measured at 20 K, and the bulk spectrum is identical for short- or long-chain F8BT. Clearly, the long-chain and bulk spectra are quite similar. This suggest that in the bulk film, regardless of the individual chain length, interchain contacts efficiently funnel the energy to red sites, so intrachain contacts are not required.

4.2 Size-Dependent Spectroscopic Properties of MEH-PPV Nanoparticles

Figure 3.6(a) shows a fluorescence image of MEH-PPV nanoparticles – because this image is indistinguishable from an image of single MEH-PPV molecules, the nanoparticles must be smaller than the resolution of our instrument. This resolution is dedicated by the diffraction limit of the excitation light used, which is ∼300 nm.

Discussion

Figure 3.6(b) shows the distribution of estimated particles sizes for nanoparticles and single molecules; the method for determining these estimates is described on page 38.

As shown in Figure 3.6(c), the emission spectra of the aggregates do not depend on their external environments – nanoparticles dissolved in water and in the polymer host PVA show essentially identical emission spectra. This suggests that the fluorescence of MEH-PPV nanoparticles is dominated by their cores; that is, the region of the nanoparticle which is not exposed to the surrounding environment and thus is insensitive to changes in it.

Another important result in Figure 3.6(c) is the comparison of these emission spectra to the emission of MEH-PPV single molecules dissolved in THF. THF is a good solvent for MEH-PPV; when dissolved in it, MEH-PPV single polymer chains "stretch out" so that they can be effectively solvated along the entire length of the chain. The result is that the intrachain contacts discussed above are absent in THF, and so the molecules essentially emit only in the blue form.

Figure 3.7 shows the distribution of peak energy as a a function of increasing particle size; from approximately $186,000$ amu in panel (a) to large aggregates of $\sim$100 such molecules. From (a) to (c), it can be seen that the number of red sites increases relative to the number of blue sites as molecular weight increases – this is a result of the effect discussed earlier in F8BT.

When multiple chains are aggregated together, the bimodal distribution collapses completely to only the red form. Similar to the bulk film F8BT measurements, this is a

result of interchain contacts in the mass of MEH-PPV molecules; in fact, as shown in Figure 3.7(f), the emission spectra of the aggregates are quite similar to measurements of bulk MEH-PPV thin films. In detailed studies, it was shown that even smaller nanoparticles exhibit this collapse to lower energy; bulk-like structural properties seem to be achieved for particles with radii greater than ∼10 nm.

The complete absence of blue sites in the emission of the multichain-assembled nanoparticles strongly suggests that there is a large increase in both the number and concentration of red sites for this form of MEH-PPV. In addition, the extreme narrowing of the emission maxima histogram suggests the presence of a large concentration of red sites with a narrow distribution of emission energies. Apparently, the assembly process in multichain-assembled nanoparticles involves a cooperative formation of red sites, probably through interchain interactions. It may be that the assembly and growth methods associated with the precipitation method used herein in fact favor the formation of red sites.

It is interesting to compare the width of the peak in the emission maxima histogram for the assembled nanoparticles to the corresponding red site peak in the smaller single-molecule particles. The broader width in the latter case has been shown previously to be due to a weak component of blue site emission that tends to shift the emission maxima of the molecules with primarily red emission and conformational heterogeneity from molecule to molecule.[9]

The narrow width of the peak for the assembled nanoparticles is further indication that essentially no detectable blue emission is present in these particles, and also suggests that

energy funneling among red sites may be operating, ensuring nearly identical emission maxima for all particles. Both of these observations are consistent with a large number of red sites per assembled nanoparticle capable of intra-site energy transfer.

References

[1] Barbara, P. F.; Gesquiere, A. J.; Park, S.-J.; Lee, Y. J. *Acc. Chem. Res.* **2005**, *38*, 612–610.

[2] Hide, F.; Díaz-García, M. A.; Schwartz, B. J.; Heeger, A. J. *Acc. Chem. Res.* **1997**, *30*, 430–436.

[3] Grey, J. K.; Lee, Y. J.; Gutierrez, J. J.; Luong, N.; Ferraris, J. P.; Barbara, P. F. *Angew. Chem. Int. Ed.* **2005**, *44*, 6207–6210.

[4] Atkins, P.; Friedman, R. *Molecular Quantum Mechanics*, 4th ed.; Oxford University Press: New York, 2005; pp 386–387.

[5] Hu, D. H.; Yu, J.; Wong, K.; Bagchi, B.; Rossky, P. J.; Barbara, P. F. *Nature* **2000**, *405*, 1030–1033.

[6] Grey, J. K.; Kim, D. Y.; Donley, C. L.; Miller, W. L.; Kim, J. S.; Silva, C.; Friend, R. H.; Barbara, P. F. *J. Phys. Chem. B* **2006**, *110*, 18898–18903.

[7] Lammi, R. K.; Barbara, P. F. *Photochem. Photobiol. Sci.* **2005**, *4*, 95–99.

[8] Yu, J.; Hu, D.; Barbara, P. F. *Science* **2000**, *289*, 1327–1330.

[9] Kim, D. Y.; Grey, J. K.; Barbara, P. F. *Synth. Meth.* **2006**, *156*, 336–345.

[10] Grey, J. K.; Kim, D. Y.; Norris, B. C.; Miller, W. L.; Barbara, P. F. *J. Phys. Chem. B* **2006**, *110*, 25568–25572.

[11] Bernius, M. T.; Inbasekaran, M.; O'Brien, J.; Wu, W. *Adv. Mater.* **2000**, *12*, 1737–1750.

[12] Kim, D. Y.; Grey, J. K.; Barbara, P. F. *Synth. Met.* **2006**, *156*, 336–345.

[13] Szymanski, C.; Wu, C.; Hooper, J.; Salazar, M. A.; Perdomo, A.; Dukes, A.; McNeill, J. D. *J. Phys. Chem. B* **2005**, *109*, 8543–8546.

[14] Wu, C.; Peng, H.; Jiang, Y.; McNeill, J. *J. Phys. Chem. B* **2006**, *110*, 14148–14154.

[15] Donley, C. L.; Zaumseil, J.; Andreasen, J. W.; Nielsen, M. M.; Sirringhaus, H.; Friend, R. H.; Kim, J.-S. *J. Am. Chem. Soc.* **2005**, *127*, 12890–12899.

[16] Rønne, C.; Trägårdh, J.; Hessman, D.; Sundström, V. *Chem. Phys. Lett.* **2004**, *388*, 40–45.

[17] Yu, Z.; Barbara, P. F. *J. Phys. Chem. B* **2004**, *108*, 11321–11326.

[18] Huser, T.; Yan, M.; Rothberg, L. J. *Proc. Natl. Acad. Sci.* **2000**, *97*, 11187–11191.

[19] Wachsmann-Hogiu, S.; Peteanu, L. A.; Liu, L. A.; Yaron, D. J.; Wildeman, J. *J. Phys. Chem. B* **2003**, *107*, 5133–5143.

[20] Zhang, H.; Lu, X.; Li, Y.; Ai, X.; Zhang, X.; Yang, G. *J. Photochem. Photobiol., A* **2002**, *147*, 15–23.

[21] Chang, R.; Hu, J.-H.; Fann, W.-S.; Yu, J.; Lin, S.-H.; Lee, Y.-Z.; Chen, S.-A. *Chem. Phys. Lett.* **2000**, *317*, 153–158.